FIG 4-3 THIRD INTERRUPTION

CARBON LOADED TO 59% OF ITS EQUILIBRIUM VALUE

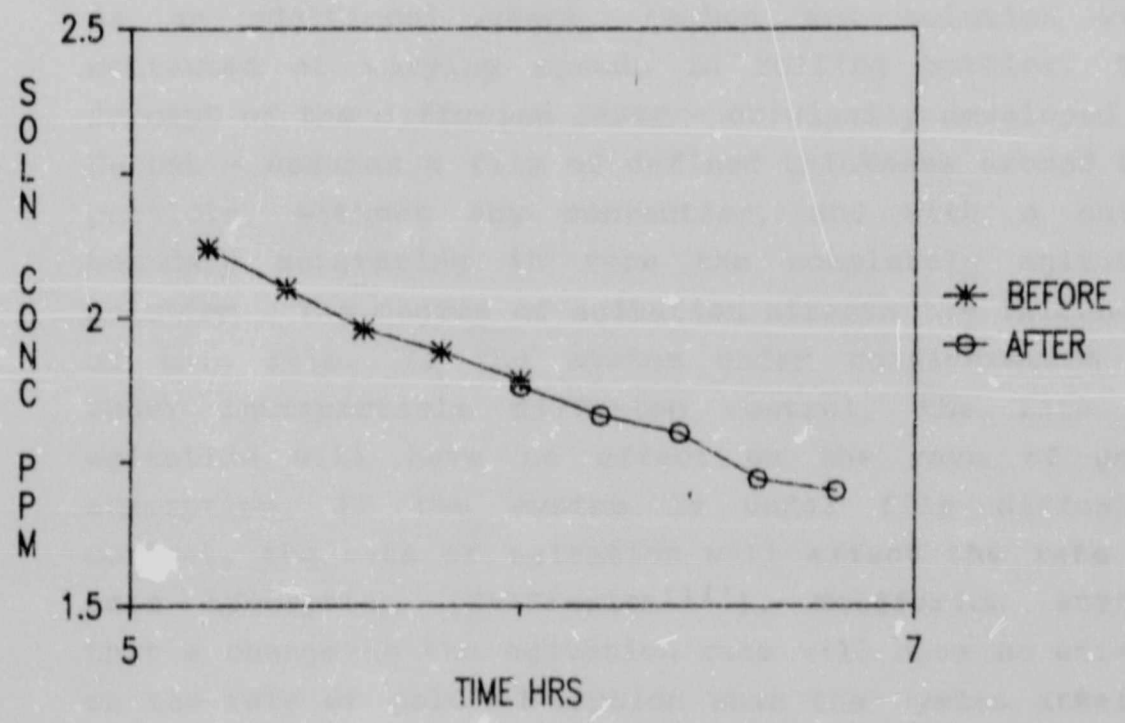

FIG 4-4 FOURTH INTERRUPTION

CARBON LOADED TO 94 % OF ITS EQUILIBRIUM VALUE

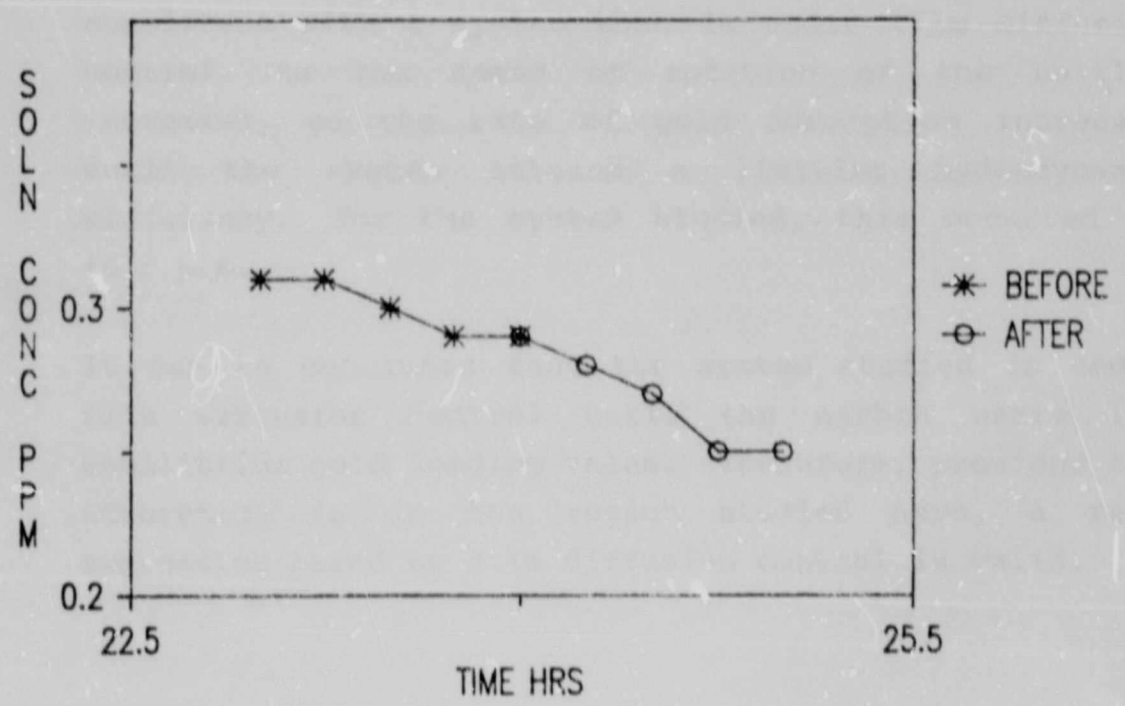

As an additional check, carbon and solution were contacted at varying speeds in rolling bottles. The concept of the diffusion layer - originally developed by Nernst - assumes a film of defined thickness around the particle, without any convection, and with a sharp boundary separating it from the completely agitated solution. The degree of agitation affects the thickness of this film. If the system under consideration is under intraparticle diffusion control, the rate of agitation will have no effect on the rate of gold adsorption. If the system is under film diffusion control, the rate of agitation will affect the rate of gold adsorption (Helfferich[12]). Helfferich states that a change in the agitation rate will have no effect on the rate of gold adsorption when the system attains its limiting hydrodynamic efficiency.

Five adsorption tests were completed at rolling bottle speeds of between 6,7 and 69,2 r.p.m., the results of which are plotted in Figure 4.5. Examination of Figure 4.5 shows that the gold adsorption profiles are consistent with a system that is under film diffusion control. As the speed of rotation of the bottles increases, so the rate of gold adsorption increases until the system attains a limiting hydrodynamic efficiency. For the system studied, this occurred at 46 r.p.m.

It can be concluded that the system studied is under film diffusion control until the carbon nears its equilibrium gold loading value. Therefore, provided the adsorption is in the region studied here, a rate expression based on film diffusion control is valid.

FIG 4--5 THE EFFECT OF ROLLING BOTTLE SPEED

ON THE RATE OF ADSORPTION

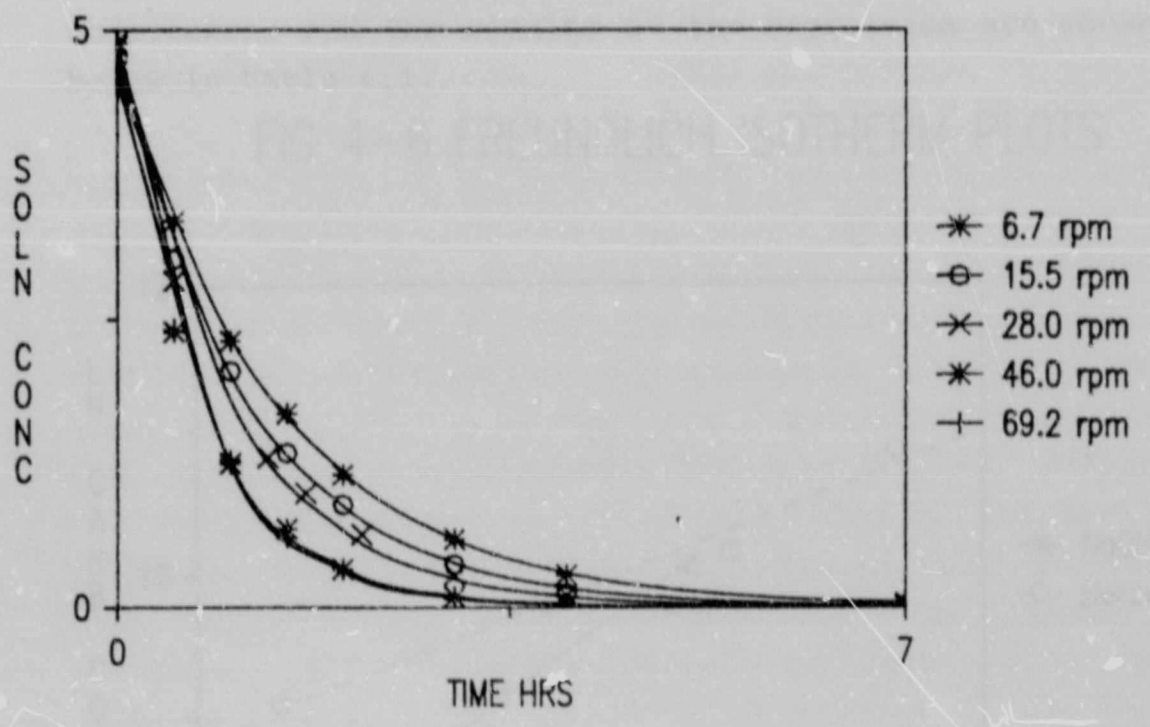

4.3 *THE EQUILIBRIUM CURVE*

McDougall[5] quotes Allen as stating that the equilibrium adsorption of gold cyanide can be described by the Freundlich isotherm. Cho[11], van Deventer[14], and Hussey[15], also assume that the Freundlich isotherm describes the equilibrium between gold in solution and gold on the carbon.

Tne Freundlich isotherm states that:

$$C_s^e = a\ (C_c^e)^b \qquad 2\text{-}4$$

where a and b are constants.

Hence, a plot of ln C_s^e versus ln C_c^e should produce a straight line of slope b and intercept ln a.

For the equilibrium tests undertaken, the Freundlich plot of ln C_s versus ln C_c was drawn and is shown in Figure 4.6. Linear regression on the resulting data was undertaken, and the results of the regression are shown below in Table 4.1.

FIG 4-6 FREUNDLICH ISOTHERM PLOTS

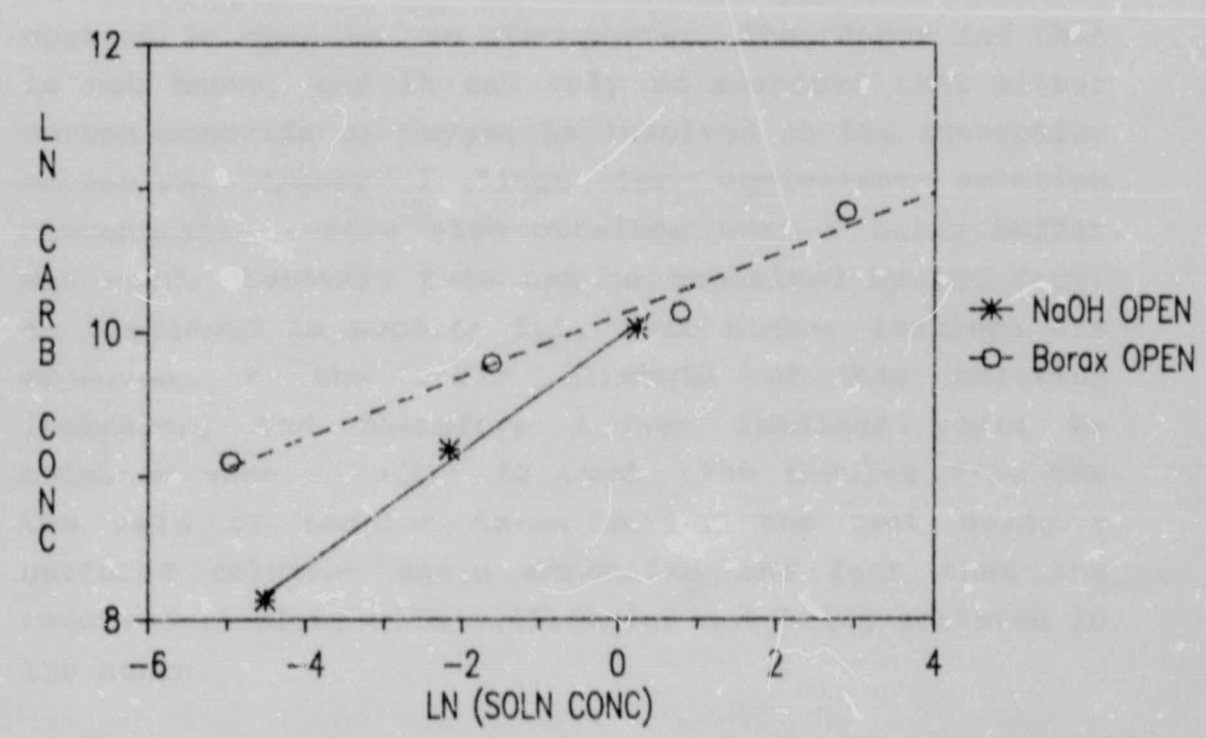

TABLE 4.1 Linear regression on equilibrium test data using Freundlich isotherms

Test	*a*	*b*	Correlation coefficient
Closed; sodium hydroxide	$1,37 \times 10^{-11}$	2,51	0,997
Open; sodium hydroxide	$3,69 \times 10^{-12}$	2,60	1,000
Open; borax t = 120 hrs	$5,58 \times 10^{-21}$	4,61	0,989
Open; borax t = 216 hrs	$8,81 \times 10^{-21}$	4,54	0,993

The graphical representation and the regression correlation coefficients show that the Freundlich isotherm adequately fits the equilibrium adsorption of gold cyanide onto carbon.

Higher equilibrium gold loadings on the carbon for equivalent solution concentrations are obtained when the contact is open to the atmosphere. The reason for this is not known, and it can only be surmised that either carbon monoxide or oxygen is involved in the adsorption mechanism. Higher loadings for equivalent solution concentrations were also obtained when a borax buffer was used. However, this can be explained by the fact, as discussed in Section 1.4, that higher loadings are expected as the ionic strength of the solution increases, and therefore higher loadings would be obtained when a buffer is used. The results from the two sets of samples taken during the test using a buffered solution again emphasise the fact that the reaction is slow, with equilibrium not being achieved in 120 hours.

Experience gained during the equilibrium tests indicated that the equilibrium is extremely sensitive, and utmost care must be exercised when doing equilibrium tests, especially at lower solution concentrations, where reaching equilibrium seems to take longer. At lower concentrations, analytical errors can cause poor linear fits.

4.4 *THE SIMULATION OF BATCH TESTS AT DIFFERENT CARBON MASSES*

The model developed needed experimental verification. This set of tests involved contacting different masses of carbon with gold-bearing solution in rolling bottles (see Section 3.5 for experimental procedure). The resulting profiles were used to calculate the mass transfer coefficients and verify the model developed.

In Section 2.3, the method of obtaining the mass transfer coefficient was discussed, namely, by varying the value of the coefficient to obtain the minimum value of the sum of the square of the errors between the predicted and observed values. For the five tests done during this phase, the graph of the mass transfer coefficient against the sum of the squares is shown in Figure 4.7, from which it can be seen that this minimum is distinct and only has a single value. The value of the sum of the squares is a measure of the fit.

FIG 4-7 MINIMIZATION OF THE SSQ

TESTWORK G , THE SUM OF SQUARES AGAINST THE COEFFICIENT

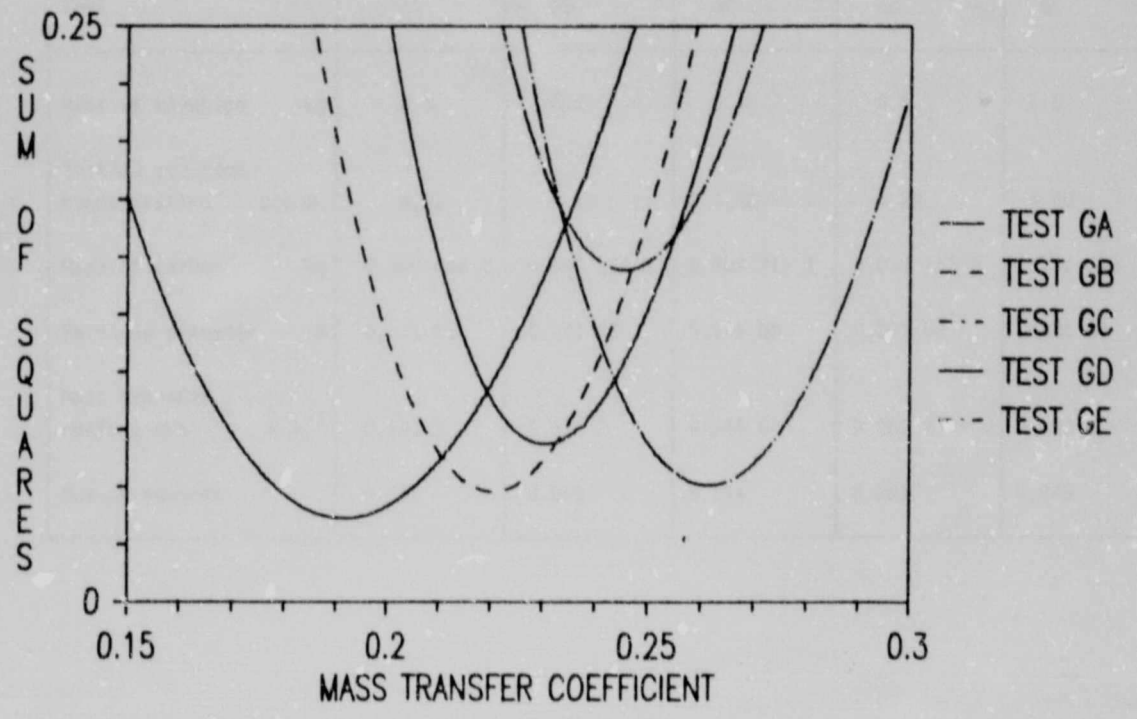

To verify the mathematics developed up to this stage, it was necessary to establish the values of the equilibrium constants and the mass transfer coefficient. The equilibrium constants were determined in Section 4.3, and the mass transfer coefficients can either be read from the plots in Figure 4.7 or established by using the program detailed in Appendix B. The numerical values of the parameters are shown in Table 4.2. The values of the sum of the squares, with the exception of Test GC, are less than 0,1, indicating a good fit.

As the ratio of carbon mass to solution volume has no effect on the value of the mass transfer coefficient, the mass transfer coefficients for all the batch tests should have equal values. Comparison shows that the values are essentially equal, with the exception of Test GA, which has a slightly lower value.

TABLE 4.2 Results from testwork at different solution-carbon ratios

Test	GA	GB	GC	GD	GE
Mass of solution kg	0,5	0,5	0,5	0,5	0,5
Initial solution concentration p.p.m.	4,32	4,26	4,28	4,28	4,40
Mass of carbon kg	0,000 062 2	0,000 124 8	0,000 211 1	0,000 353 6	0,000 643
Particle diameter m	0,001 85	0,001 85	0,001 85	0,001 85	0,001 85
Mass transfer coefficient $m\ h^{-1}$	0,191 9	0,220 7	0,245 6	0,261 6	0,230 6
Sum of squares	0,036	0,048	0,144	0,051	0,069

In order to present the data, the predicted profiles are superimposed on the observed points. The predicted solution profiles were obtained by the use of Equation 2-9, which is the expression describing the concentration of solution with time, given in Section 2.2 A mass transfer coefficient value of 0,230 m h^{-1} was used, which is the average value. The plots of the observed and predicted data are given in Figure 4.8, and it can be observed that the predicted lines fit the observed data adequately.

FIG 4-8 MODEL FITS OF TEST G

PREDICTED LINES AND OBSERVED DATA

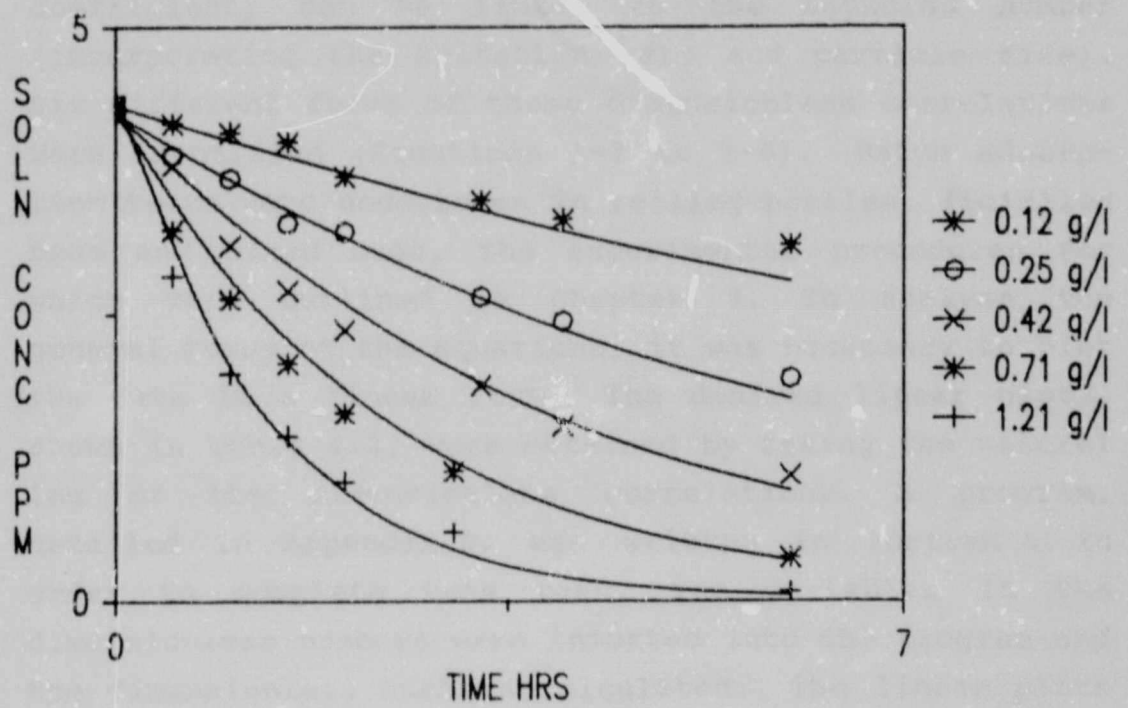

4.5 MASS TRANSFER COEFFICIENT CORRELATIONS

4.5.1 Introduction

In Section 2 a rate expression was proposed which included equilibrium constants and a mass transfer coefficient, and the method of obtaining these parameters was outlined. As discussed in Section 1.4, no work has been published on mathematically relating the rate of gold adsorption to the system parameters affecting the rate, namely, the particle size and the agitation rate. However, in Section 1.4, the literature relating the mass transfer coefficient to these system parameters was reviewed, and this revealed that the Sherwood number (incorporating the mass transfer coefficient) can be linked to the Reynolds number (incorporating the agitation rate and particle size). Six different forms of these dimensionless correlations were identified (Equations 1-1 to 1-6). Batch adsorption tests were undertaken in rolling bottles, fluidized beds and fixed beds, the experimental procedures for which were outlined in Chapter 3. To analyse the general forms of the equations, it was necessary to plot the data in a linear form. The desired linear plots, shown in Table 4.3, were obtained by taking the natural log of the dimensionless correlations. A program, detailed in Appendix D, was written in Fortran 5 in order to complete this task. The variables in the dimensionless numbers were inputted into the program and the dimensionless numbers calculated. The linear plots were drawn, and the program outputted the slope, the intercept, and the linearly regressed correlation coefficient for each of the six equations.

TABLE 4.3 Plotting of the dimensionless numbers to obtain straight lines

Equation	x axis	y axis	Slope	Intercept
1-1	$\ln Re$	$\ln \frac{Sh - 2}{Sc^{0,33}}$	q	$\ln p$
1-2	$\ln Re$	$\ln \frac{Sh \cdot \epsilon}{Sc^{0,33}}$	q	$\ln p$
1-3	$\ln (1-\epsilon)Re$	$\ln \frac{Sh \cdot \epsilon}{Sc^{0,33}}$	q	$\ln p$
1-4	$\ln (1-\epsilon)Re$	$\ln \frac{Sh - 2}{Sc^{0,33}}$	q	$\ln p$
1-5	$\ln Re$	$\ln \frac{Sh}{Sc^{0,33}}$	q	$\ln p$
1-6	$\ln (1-\epsilon)Re$	$\ln \frac{Sh}{Sc^{0,33}}$	q	$\ln p$

The procedure followed to analyse the raw experimental data was as follows:

* The equilibrium concentrations, and hence the equilibrium constants, were calculated using the method outlined in Section 2.3.

* The mass transfer coefficient was then obtained by the method outlined in Section 2.3 and using the program detailed in Appendix B.

* Using these variables, the dimensionless numbers were calculated for each batch test. The determination of the variables is given in Appendix C.

* All six suggested dimensionless correlations were then tested on the dimensionless numbers to obtain the best fit relationship. The program detailed in Appendix D was used to obtain the constants and regression correlation coefficients for Equations 1-1 to 1-6.

* The best fitting dimensionless number correlation was then proposed as the relationship that holds for the system under consideration. The mass transfer coefficient for a few of the batch tests was then calculated by means of the proposed relationship, and the predicted curves using Equation 2-9 were plotted with the observed data.

4.5.2 The fluidized bed

Fleming [8] established the fact that, whilst the pH value of the solution has a slight effect on the rate, it has a considerable effect on the capacity of the carbon. The pH value of the solution was monitored during the runs and was found to remain constant, indicating that the borax buffer concentration was sufficient to offset the natural acidity of the carbon.

The results from manipulation of the data to obtain the mass transfer coefficients are shown in Table 4.4. For the convenience of the reader, the coefficients are given as units of m h^{-1} instead of m s^{-1}. They vary from 0,111 to 0,179 m h^{-1}. The sum of the squares of the errors from the non-linear regression is less than 0,10, except in the case of Tests EB and EK.

TABLE 4.4 Mass transfer coefficients for fluidized bed tests

Test	Initial soln concn p.p.m.	Mass of carbon kg	Mass transfer coefficient m h^{-1}	Sum of squares
EA	4,21	0,007 948	0,179 8	0,054
EB	4,59	0,007 948	0,164 8	0,289
EC	3,62	0,007 948	0,143 9	0,045
ED	3,34	0,007 948	0,111 1	0,064
EE	3,71	0,007 676	0,167 2	0,062
EF	3,64	0,007 676	0,139 0	0,064
EG	3,58	0,007 728	0,155 9	0,051
EH	,52	0,007 728	0,143 7	0,060
EI	3,46	0,007 676	0,149 1	0,065
EJ	3,45	0,007 728	0,156 1	0,051
EK	4,07	0,007 948	0,133 8	0,335
EL	4,07	0,007 948	0,178 6	0,059
EM	4,14	0,007 728	0,165 9	0,087
EN	4,14	0,007 728	0,165 3	0,100

For all tests - Mass of solution = 20 kg
Freundlich *a* = $8,812 \times 10^{21}$
Freundlich *b* = 4,538

The dimensionless numbers for each test were calculated and the results are given in Table 4.5 All three carbon size fractions were used during the tests, and the linear velocity through the column varied from 0,009 to 0,023 m s^{-1}. (The linear velocity is defined as the area of the column divided by the solution flowrate, as set out in Appendix C, that is, the linear velocity is the superficial velocity.) The variation of the linear velocity resulted in the variation of the voidage from 0,59 (5 per cent bed expansion) to 0,73 (57 per cent bed expansion). The Reynolds numbers varied from 19,6 to 49,9. The Sherwood numbers varied from 61,9 to 109,7.

Equations 1-1 to 1-6 were used to analyse the effects of linear velocity and particle diameter on the mass transfer coefficients. The plots listed in Table 4.3 were drawn and the slopes and linear regression coefficients obtained. The results appear in Table 4.6.

Table 1.1 listed the correlations, derived from the literature, linking the Reynolds number, the Sherwood number and the Schmidt number. The investigators quoted, with the exception of two, gave the power of the Reynolds number as 0,5. The equation which gives the highest correlation coefficient, as well as q in the vicinity of 0,5, is Equation 1-2, which was derived from work done by Snowdon[22] and Rahman[23]. Their investigations were carried out on ion exchange resins in fluidized and fixed beds.

The plot of ln Re against ln $(Sh \cdot \epsilon / Sc^{0,33})$ is shown in Figure 4.9 If Equation 1-2 holds, this plot should be linear. The linear regression coefficient of this plot is 0,96.

TABLE 4.5 Dimensionless numbers for fluidized bed tests

Test	Particle diameter m	Linear velocity m s^{-1}	Voidage	Reynolds number	Sherwood number
A	0,002 18	0,023	0,73	49,9	109,7
B	0,002 18	0,010	0,59	20,7	99,7
C	0,002 18	0,016	0,66	33,8	87,2
D	0,002 18	0,012	0,62	26,2	67,2
E	0,001 85	0,017	0,69	31,5	85,8
F	0,001 85	0,011	0,62	20,9	71,3
G	0,001 55	0,017	0,71	26,4	67,2
H	0,001 55	0,011	0,66	17,5	61,9
I	0,001 85	0,013	0,64	23,1	76,7
J	0,001 55	0,015	0,70	23,6	67,2
K	0,002 18	0,009	0,59	19,6	81,1
L	0,002 18	0,009	0,59	19,8	108,1
M	0,001 55	0,018	0,72	28,2	71,4
N	0,001 55	0,016	0,70	24,0	71.1

NOTE: For all tests -

1. The Schmidt number = 1000
2. The density = 1000 kg m^{-3}
3. The viscosity = 0,001 kg m^{-1} s^{-1}
4. The diffusivity = 10^{-9} m^2 s^{-1}

TABLE 4.6 Fitting dimensionless number correlations for the fluidized bed

Relationship tested	Correlation coefficient	q
4-1	0,80	0,44
4-2	0,90	0,57
4-3	0,79	0,60
4-4	0,86	0,57
4-5	0,80	0,44
4-6	0,86	0,57

FIG 4-9 FLUIDIZED BED DIMENSIONLESS NUMBER FIT
PLOTTING OF LN(Re) versus LN((Sh. ϵ)/(Sc**1/3))

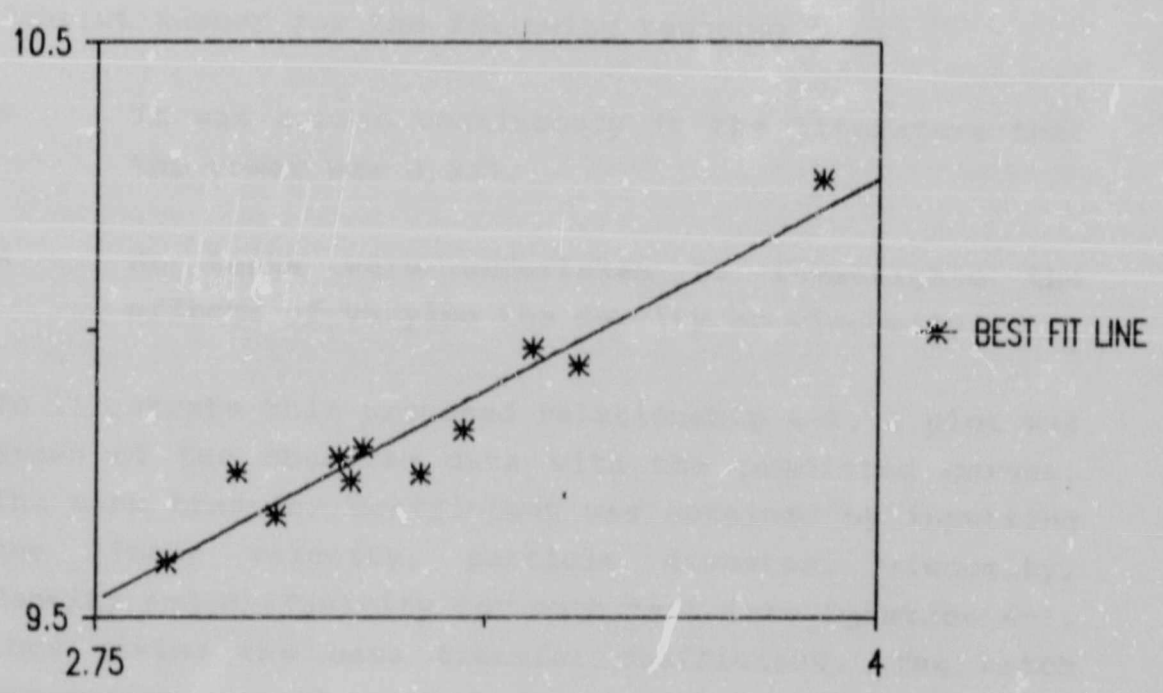

Therefore it is proposed that the relationship linking dimensionless numbers is

$$Sh = \frac{0,754}{\epsilon} Re^{0,589} Sc^{0,333} \qquad 4\text{-}1$$

The relationship proposed by Rahman[23] is

$$Sh = \frac{0,86}{\epsilon} Re^{0,5} Sc^{0,33}$$

and the relationship proposed by Snowdon[22] is

$$Sh = \frac{0,81}{\epsilon} Re^{0,5} Sc^{0,33}$$

Because these investigators also carried out their work on adsorption, the relationship proposed above agrees with their findings.

No work was undertaken to establish the power of the Schmidt number for the following reasons:

* It was agreed unanimously in the literature that the power was 0,333.

* No tests were undertaken to investigate the effects of varying the density or viscosity.

To illustrate this proposed relationship 4-1, a plot was drawn of the observed data with the predicted curves. The mass transfer coefficient was obtained by inputting the linear velocity, particle diameter, viscosity, density and diffusivity for each test into Equation 4-1, thus giving the mass transfer coefficient. The batch expression was then used to obtain the rate of gold leaving the solution with time, that is, the mass transfer coeffient, equilibrium constants, mass of carbon, mass of solution, initial solution concentration, initial carbon concentration, and the area of the carbon, were inputted into Equation 2-9 and solved. Three batch tests were chosen from the work done on the adsorption of gold from a fluidized carbon bed:

* Test EK. In this test the largest carbon size fraction was used, at a low linear velocity. This should produce slow kinetics.

* Test EN. In this test the smallest carbon size fraction was used, at a high linear velocity. This should produce fast kinetics.

* Test EI. In this test the medium carbon size fraction was used, at an intermediate velocity. This should produce kinetics between the above two examples.

The parameters and constants for each of the three tests are given in Table 4.7. Figure 4.10 shows the plot of the observed data and the curves predicted by Equations 4-1 and 2-9. Visual observation of the plots shows good fits for Tests EN and EI, while for Test EK the predicted kinetics are slower than the observed kinetics.

TABLE 4.7 Fluidized bed examples for predicted curves against observed data

Test		EK	EN	EI
Particle diameter	m	0,002 18	0,001 55	0,001 85
Linear velocity	$m\ s^{-1}$	0,009	0,015 5	0,012 5
Mass of carbon	kg	0,007 95	0,007 73	0,007 68
Reynolds number		19,6	24,0	23,1
Sherwood number		73,6	70,0	75,0
Mass transfer coefficient	$m\ h^{-1}$	0,122	0,163	0,146
Voidage		0,59	0,70	0,64

NOTE:

Mass of solution	=	20 kg
Schmidt number	=	1000
Initial carbon concentration	=	0 $mg\ kg^{-1}$
Diffusivity	=	$10^{-9}\ m^2\ s^{-1}$
Viscosity	=	0,001 $kg\ m^{-1}\ s^{-1}$
Density	=	1000 $kg\ m^{-3}$
Freundlich *a*	=	$8,812 \times 10^{-21}$
Freundlich *b*	=	4,538

It can therefore be concluded that the effects of particle diameter and linear velocity in a fluidized carbon bed can be linked to the mass transfer coefficient via dimensionless numbers.

FIG 4–10 FLUIDIZED BED MODEL FITS

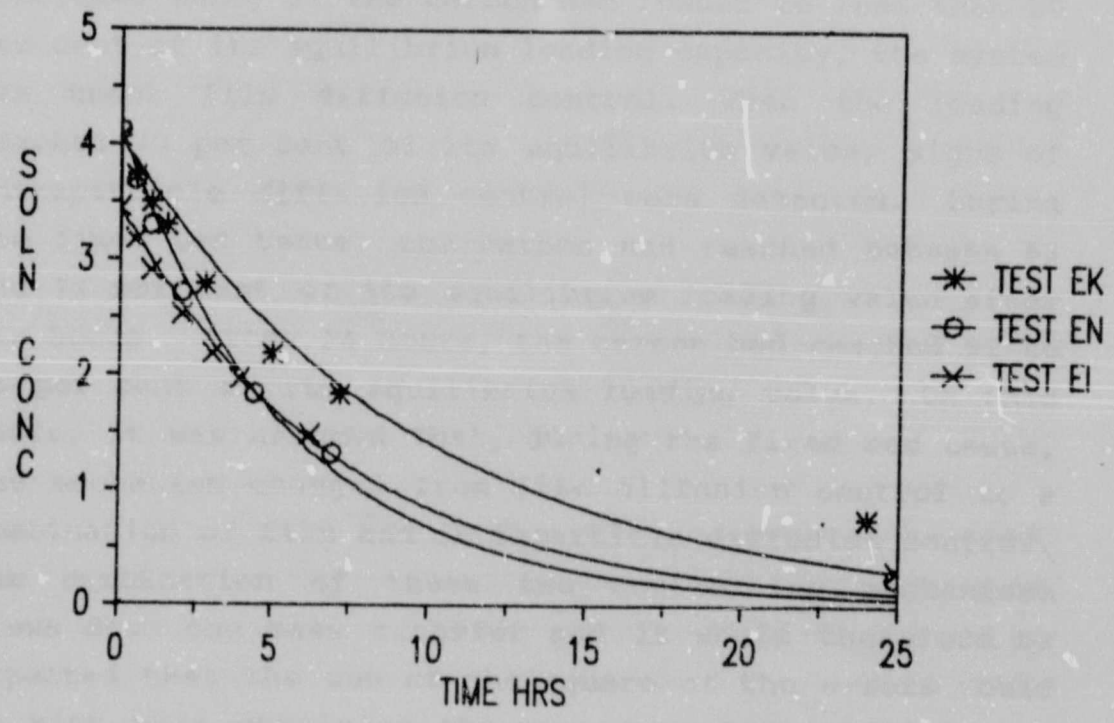

4.5.3 The fixed bed

The same procedure as that for the fluidized bed tests was followed in analysing the results of the fixed bed tests, namely, the equilibrium constants were calculated, the mass transfer coefficients were obtained, the dimensionless number plots were drawn, an equation was proposed, and the predicted curves were shown for a few isolated tests.

The results from the manipulation of the data to obtain the mass transfer coefficients are given in Table 4.8. The mass transfer coefficients varied from 0,20 to 0,30 m h^{-1}. The sum of the square of the errors from the non-linear regression was greater than 0,01, whereas, in order to indicate an excellent fit, it is desirable to have an error of less than 0,01. The reason for these errors was as follows:

During the interruption tests (Section 4.2), it was concluded that, if the carbon had loaded to less than 60 per cent of its equilibrium loading capacity, the system was under film diffusion control. When the loading reached 90 per cent of its equilibrium value, signs of intraparticle diffusion control were detected. During the fixed bed tests, the carbon had reached between 63 and 73 per cent of its equilibrium loading value after six hours. After 24 hours, the carbon had reached 91 to 95 per cent of its equilibrium loading value. On this basis, it was assumed that, during the fixed bed tests, the mechanism changed from film diffusion control to a combination of film and intraparticle diffusion control. The combination of these two controlling mechanisms slows down the mass transfer and it would therefore be expected that the sum of the square of the errors would be high when obtaining the mass transfer coefficients, as the rate expression, and thus the model, is based only on film diffusion.

TABLE 4.8 Mass transfer coefficients for fixed bed tests

Test	Initial soln concn p.p.m.	Mass of carbon kg	Mass transfer coefficient $m\ h^{-1}$	Sum of squares
FA	3,96	0,007 676	0,221 9	0,195
FB	3,98	0,007 676	0,239 3	0,221
FC	4,01	0,007 948	0,263 8	0,163
FD	4,00	0,007 948	0,299 8	0,138
FE	4,06	0,007 728	0,226 3	0,202
FF	4,01	0,007 728	0,245 2	0,240
FG	4,12	0,007 948	0,202 2	0,228
FH	4,07	0,007 676	0,198 7	0.166
FI	4,35	0,007 676	0,285 9	0,297
FJ	4,30	0,007 728	0,221 7	0,359

NOTE: For all tests - Mass of solution = 20 kg
Freundlich a = $8,812 \times 10^{-21}$
Freundlich b = 4,538